Chapter 1

Trilinear Higgs Coupling

Besides measuring basic properties of newly discovered particles such as mass, decay width, branching ratios and spin-parity, it is really important to measure its couplings. Precise determination of Higgs couplings to fermions, gauge bosons and the Higgs itself, are a few of the most important experimental challenges for future experiments. Higgs self couplings are more important in order to reconstruct the Higgs potential and hence to confirm the mechanism of EWSB(Electro Weak Symmetry Breaking). The Higgs potential in the effective Lagrangian can be written as,

$$V(\phi) = -\mu^2(\phi^\dagger\phi) + \frac{1}{2}\lambda(\phi^\dagger\phi)^2 \tag{1.1}$$

Where $\lambda = \frac{M_h^2}{v^2}$ and $\mu^2 = \frac{M_h^2}{2}$. M_h is the Higgs mass, v is the vacuum expectation value and ϕ is the Higgs field. This Higgs potential basically depends on m_h and v, $v = (\sqrt{2}G_F)^{-\frac{1}{2}} \cong 246\ GeV$ and G_F is Fermi constant, which was measured over 80 years ago. m_h, the SM Higgs mass was measured few years ago by the ATLAS and CMS collaborations at the LHC it was found that $m_h = (125.09 \pm 0.24)\ GeV$[1][2]. Rewriting the Higgs potential in terms of physical Higgs boson leads to the trilinear Higgs coupling which is defined as,

$$\lambda_{hhh}^{SM} = -\frac{3m_h^2}{v} \tag{1.2}$$

The next experimental challenge remaining is to measure the Higgs self couplings in order to verify the Higgs Potential. Both the trilinear Higgs coupling(λ_{hhh}) and the quartic coupling(λ_{hhhh}) should be measured independently to determine the Higgs potential accurately. λ_{hhh} can be measured at the LHC via Higgs pair production processes explained earlier in this dissertation. In the next section we will be discussing the possibility of measuring the trilinear Higgs coupling with the improved cross section values presented here. However measuring Higgs self couplings are not an easy task at the LHC because of small cross section values and large backgrounds in the $gg \to hh$ process. Measuring couplings between three physical Higgs bosons is a priority for the proposed linear e^+e^- collider (ILC) and we will also initiate the study of Higgs production via electron positron collision.

1.1 Measuring the Trilinear Higgs coupling at LHC

As we see in Fig. 2.1 , Higgs pair production from gluon fusion involves trilinear Higgs self couplings in its triangle diagram and in the b quark fusion . Recently many groups [3] [4] [5] [6] [7] have carried out several phenomenological studies about the possibility of determining the Higgs boson self-coupling at hadron colliders. In this study, we will be discussing the possibilities of measuring trilinear Higgs coupling at the LHC using the cross sections evaluated for Higgs pair productions discussed in this thesis so far. Higgs pair production from gluon fusion via box and triangle diagrams are dominant production channels to be considered towards measuring the trilinear Higgs self coupling at LHC. Though only the triangle diagram contains the self coupling in it, the interference of the two amplitudes is sensitive to the hhh coupling. Cross sections for Higgs pair production are presented in Fig 1.1 as a function of κ, for three different center of mass energies. κ is the ratio of trilinear Higgs coupling to the standard Model trilinear higgs coupling given by equation 1.2, which is,

$$\lambda_{hhh} = \kappa \times \lambda_{hhh}^{SM} \tag{1.3}$$

In Figure 1.1 the cross sections are plotted as a function of κ for three differnt center of mass energies. As can be seen from the plot at $\kappa \approx 2.5$, the cross section has a minimum value due to the complete destructive interference from the two Feynman diagrams box and triangle. Though the shape of this curve looks the same for all channels the minimum locates in different κ values depending on the channel [7].

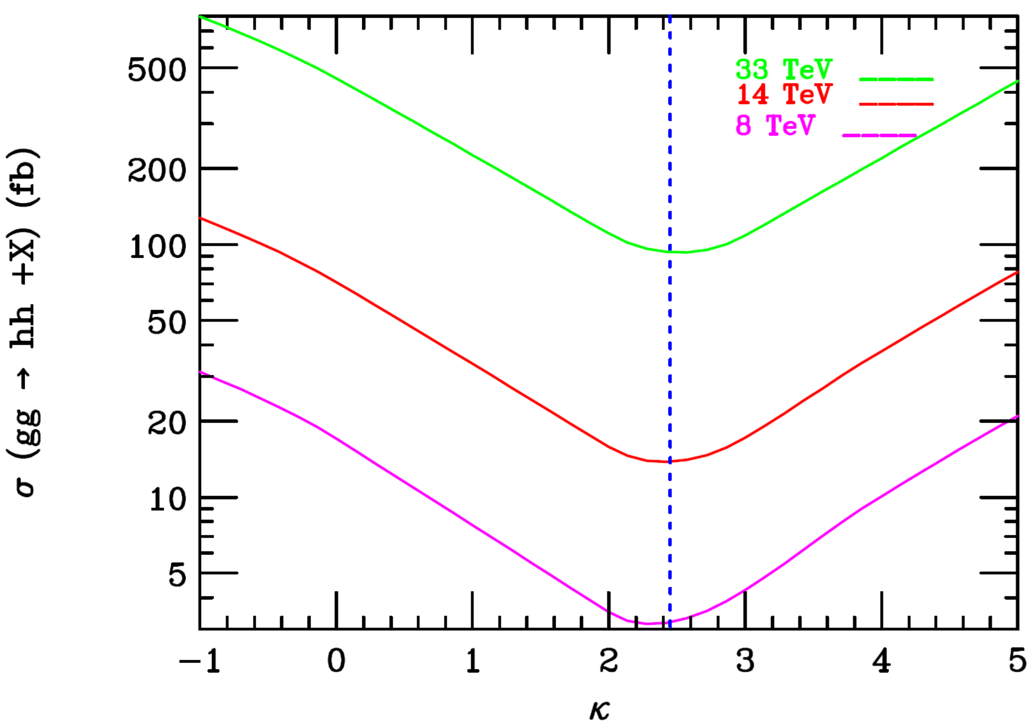

Figure 1.1: NLO(LO+kfactor(1.88)) cross sections for Higgs pair production via $gg \to hh$ as a function of κ for three different energies. No Higgs decay is considered here.

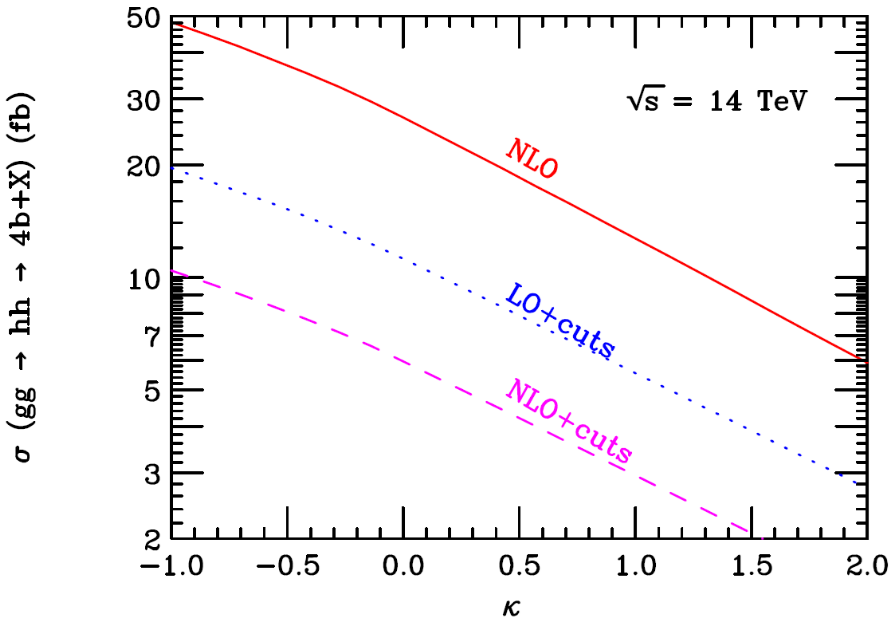

Figure 1.2: Cross section of $gg \to hh \to (b\bar{b})(b\bar{b})$ as a function of κ. The red solid line shows the NLO cross section without any cuts, the blue dotted line shows LO cross section with cuts and the dash magenta line shows NLO cross section including all cuts for the final state particles.

Figure 1.2 shows the total NLO and LO cross sections for the process $gg \to hh \to (b\bar{b})(b\bar{b})$ for the center of mass energy of 14 at LHC calculated for different κ values. The selection cuts we applied here are the same as explained in the 2nd and the 4th chapters.

The variation of significance as a function of kappa is presented in Fig. 1.3 for $\mathcal{L} = 30fb^{-1}$ and $300fb^{-1}$. The significance decreases as $\kappa = \frac{\lambda_{hhh}}{\lambda_{hhh}^{SM}}$ increases due to a reduction in the cross section. The significance for $b\bar{b}b\bar{b}$ is greatly enhanced here by introducing the mass cut which reduces a large amount of QCD backgrounds

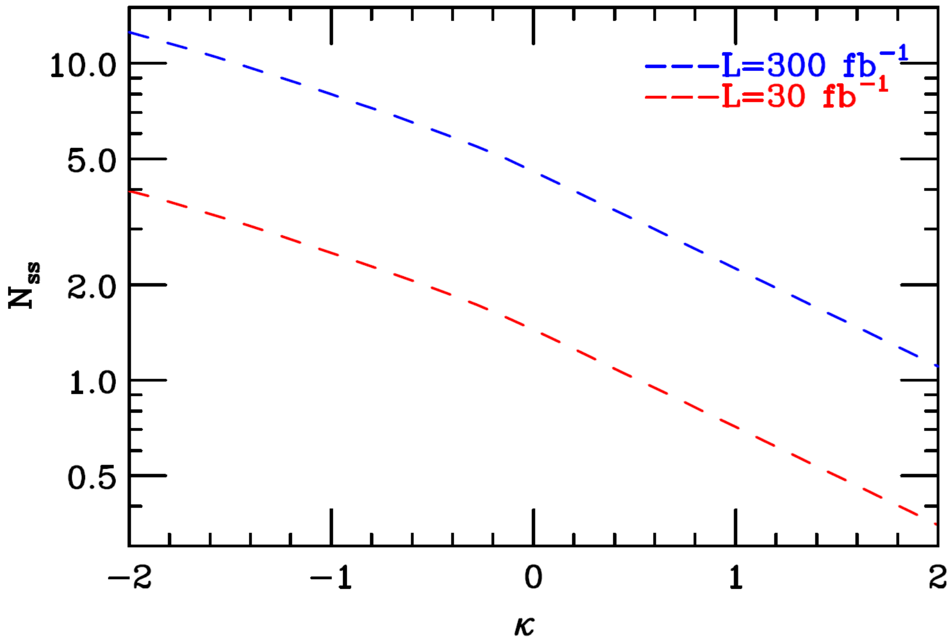

Figure 1.3: The calculated significances for the SM Higgs pair production via $gg \to hh \to (b\bar{b})(b\bar{b})$ for different values of κ at 3000 fb^{-1} for 14 TeV at the LHC.

associated with the $b\bar{b}b\bar{b}$ final state and for $\kappa = 1$ significance is $\tilde{6}.94$ for the luminosity of 3000 fb^{-1}. Also as presented in Chapter 5, the $b\bar{b}\tau^+\tau^- \to b\bar{b}lj+$ has significance of $\tilde{7}.7$. With these results we can claim that both of these channels have positive constraints towards measuring the trilinear Higgs coupling at 14 TeV LHC with integrated luminosity of 3000 fb^{-1}. Reference [6] claims that one can set a limit for $\lambda \leq 1.2$ at 95% CL for $b\bar{b}b\bar{b}$ final state at 3000 fb^{-1}. Reference [7] concludes that $b\bar{b}\tau^+\tau^-$ is a promising channel to start real experimental analysis to probe the trilinear Higgs coupling at LHC through Higgs pair production. The results of this study also verify the same fact even with high acceptance for $b\bar{b}b\bar{b}$ final state.

1.2 Measuring Trilinear Higgs coupling at ILC

Lepton colliders are well known for high precision measurements. Measuring the tri-linear Higgs coupling will be one of the main focuses for the next proposed $e^+ e^-$ machine, the International Linear collider(ILC). The ILC is an electron positron collider and planned to have a collision energy in the range 500 $GeV - 1\ TeV$. This will initially run at energies $\sqrt{s} = 200 - 500$ GeV with an integrated luminosity of 500 fb^{-1} [8] TDR-ILC. More details about the design and expected upgrades can be found in [9] [10]. Even though the collision energy for the LHC is higher than that of the ILC, measurements are expected to be more accurate at the ILC with higher luminosity.

In this study we focus on the Higgs pair production at the ILC via $e^+ e^-$ collisions -three major processes of Higgs production were studied here to explore the trilinear Higgs couplings. We assume that κ is a free parameter which is in the range $0.5 \leq \kappa \leq 2$.

Variation of cross sections were studied as a function of κ and for the collision energy changing from 500 GeV to 2 TeV using a Monte Carlo program with the amplitudes calculated by MadGraph5. Cross sections were also calculated directly from MadGraph5 for comparison purposes. Numerical values given here are calculated at the mass of the SM Higgs boson(126 GeV).

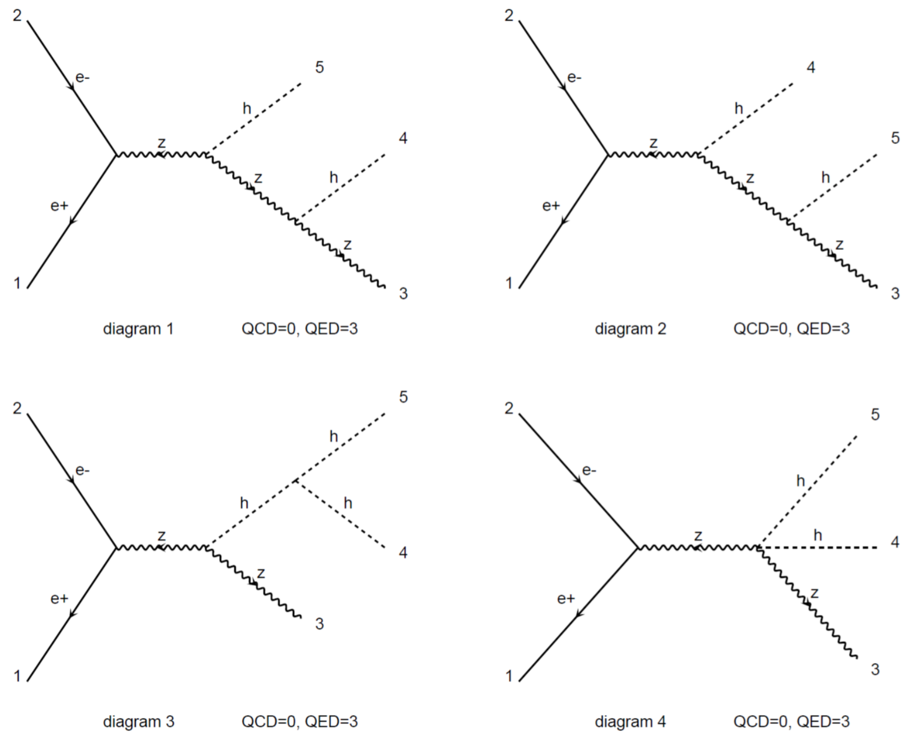

Figure 1.4: Feynman diagrams produced by MadGraph5 for the process $e^+e^- \to Zhh + X$, diagram 3 involves trilinear Higgs self coupling.

1.2.1 $e^+e^- \to Zhh + X$

$e^+e^- \to Zhh$ is one of the major processes to produce two Higgs at electron positron colliders. Several studies have been done discussing the possibility of measuring the trilinear Higgs self coupling through this process at the ILC [11][12][13]. Fig. 1.4 shows the Feynmann diagrams for the double Higgs strahlung process $e^+e^- \to Zhh + X$ which includes one diagram with the trilinear Higgs coupling and three other diagrams which does not include self coupling. We studied the cross sections as a function of κ for different center of mass energies. Fig. 1.5 presents the calculated cross sections for center of mass energies of 500 GeV, 1000 GeV and 2000 GeV. The red dashed line shown here is for the contribution over diagram 1, 2 and 4 which does not contributes to the trilinear Higgs coupling and is a constant over the ratio of $\frac{\lambda_{hhh}}{\lambda_{hhh^{SM}}}$. Blue dashed line is for the 3rd diagram which has trilinear couplings in it and the solid line represents the total cross section for all 4 diagrams.

1.2.2 $e^+e^- \to hh\nu_e\nu_e + X$

$e^+e^- \to \nu_e\overline{\nu_e}hh$ is also considered to be a dominant process for Higgs production which probes the Higgs self coupling. Higgs production via double-Higgs strahlung at linear colliders have been discussed in past studies [7] [11]. All possible Feynmann diagrams for the process $e^+e^- \to \nu_e\overline{\nu_e}hh + X$ via W and Z bosons are included in the Appendix E. There are two diagrams with the trilinear Higgs coupling and six other diagrams which have no self coupling. The contribution from WW fusion is higher compared to ZZ but here we consider combined results from both. Fig. 1.7 shows the cross section for the process as a function of $\kappa = \frac{\lambda_{hhh}}{\lambda_{hhh}^{SM}}$.

1.2.3 $e^+e^- \to hhe^+e^- + X$

As stated in Fig. 1.8, production cross sections of Higgs via $e^+e^- \to hhe^+e^- + X$ were studied as a function of κ. All possible Feynman diagrams made by MadGraph5 can be find in the Appendix.

1.2.4 Summary

The production cross sections for the processes Zhh, $\nu_e\overline{\nu_e}hh$ and hhe^+e^- as a function of center of mass energy at the Higgs mass of 126 GeV are given in Fig. 1.6. As can

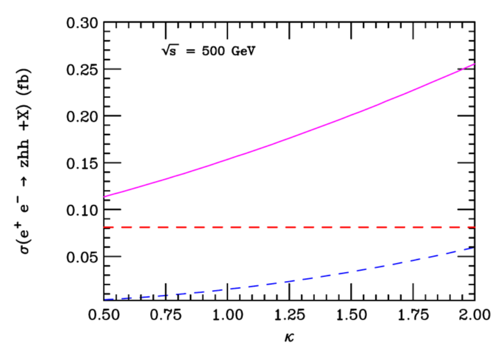

(a)

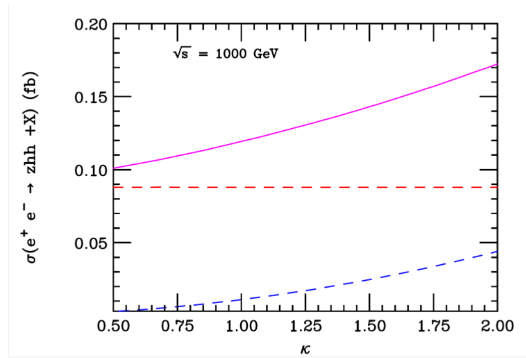

(b)

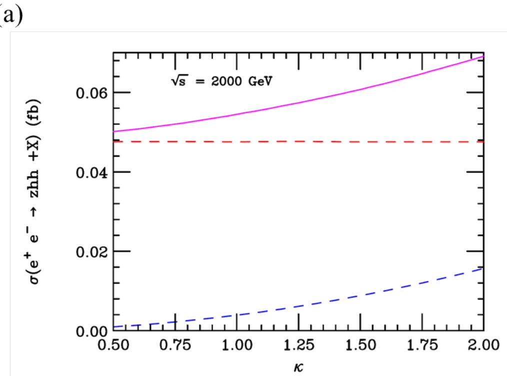

(c)

Figure 1.5: Cross section of Higgs pair production for the process $e^+e^- \to Zhh + X$ as a function of κ. Solid (magenta) represents the total cross section, red dashed line represents the contribution of diagrams with no trilinear Higgs vertex and blue dashed line represents the contribution of diagrams with trilinear Higgs vertex.

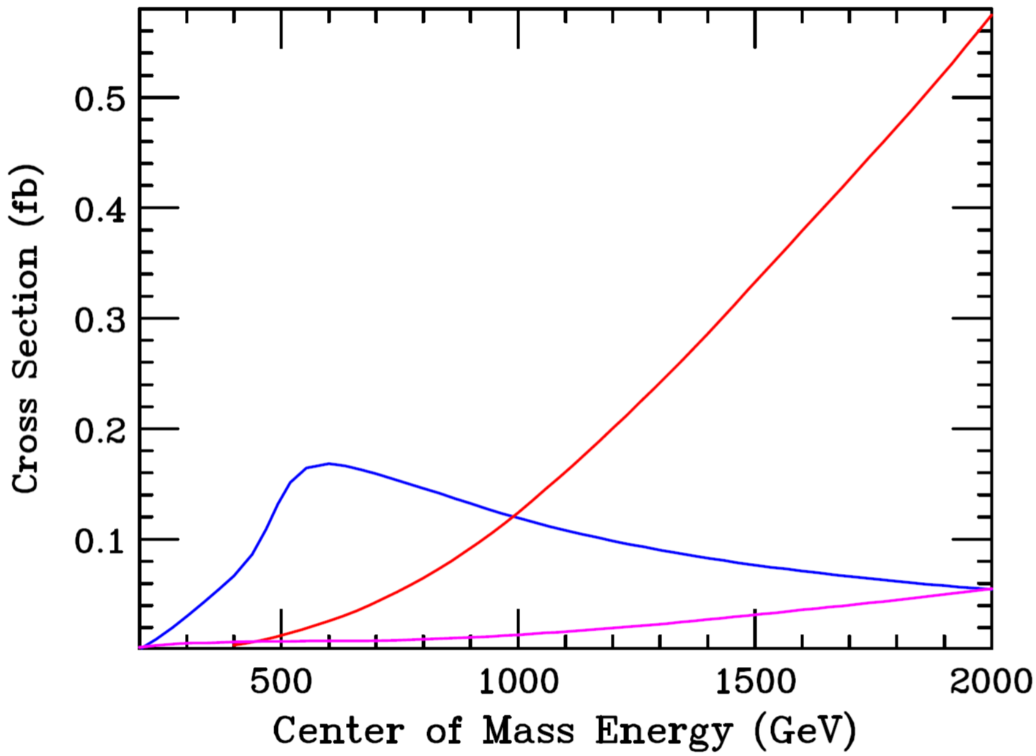

Figure 1.6: Cross sections of three major Higgs production processes at the ILC as a function of $\sqrt{s}$. The blue solid line represents zhh final state, the red line represents $\nu_e \nu_e hh$ final state and the magenta line represents e^+e^-hh final state.

be seen from the figure, the $e^+e^- \to Zhh + X$ process gives higher cross sections for lower energies around 500 GeV while $e^+e^- \to \nu\bar{\nu}hh + X$ gives higher cross sections at higher center of mass energies. The process $e^+e^- \to hhe^+e^- + X$ gives comparably lower cross sections compared to the other two processes. However, the combination of all these processes gives significantly large cross sections for overall center of mass energies. Though the cross sections produced here are smaller than the cross sections produced at the LHC for example in gluon fusion, the IlC processes are still promising since they are not covered by the large backgrounds as in LHC. As emphasized in [11] and [12] there is a possibility of measuring the trilinear Higgs self coupling even with the center of mass energy of 500 at the ILC with high luminosities.

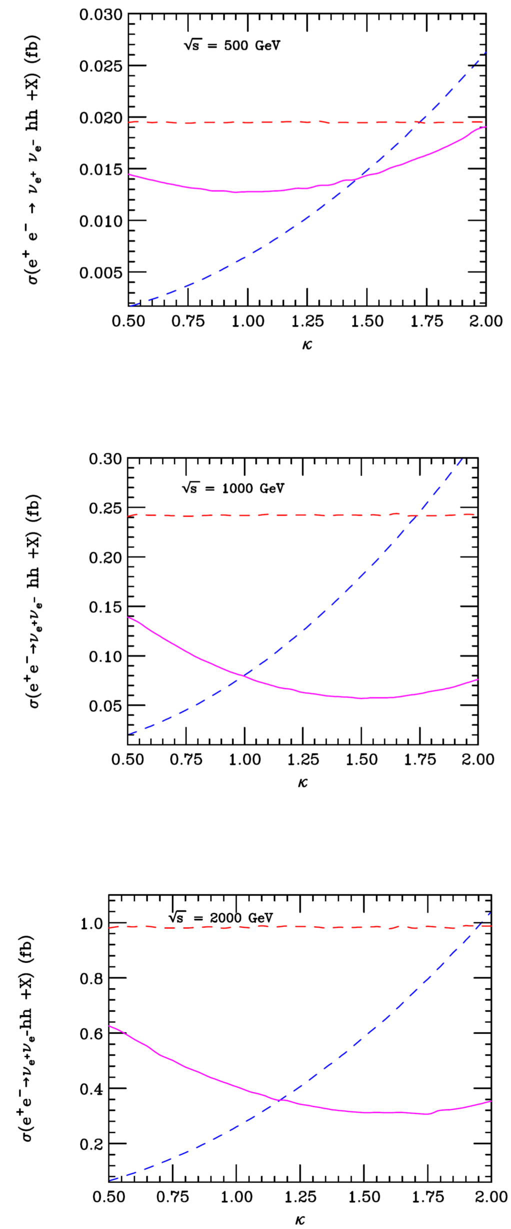

Figure 1.7: Cross section of Higgs pair production for the process $e^+e^- \to \nu_e\nu_e hh{+}X$ as a function of κ. The solid (magenta) line represents the total cross section, the red dashed line represents the contribution of diagrams with no trilinear Higgs vertex and the blue dashed line represents the contribution of diagrams with a trilinear Higgs vertex.

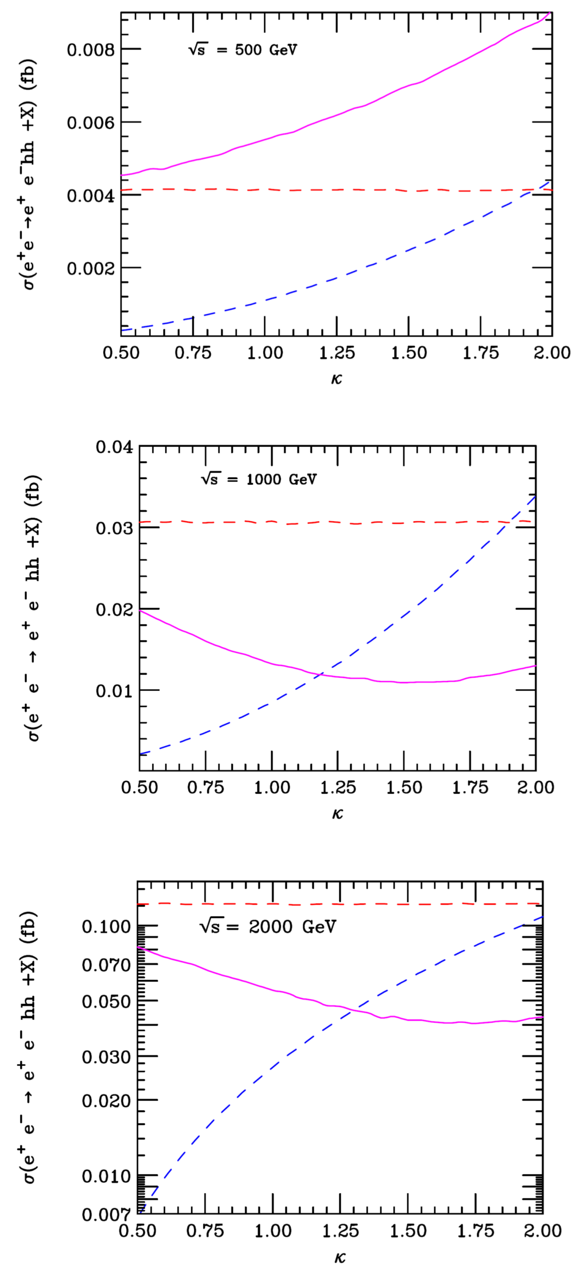

Figure 1.8: Cross section of Higgs pair production for the process $e^+e^- \to e^+e^-hh + X$ as a function of κ. The solid (magenta) line represents the total cross section, the red dashed line represents the contribution of diagrams with no trilinear Higgs vertex and the blue dashed line represents the contribution of diagrams with trilinear Higgs vertex.

References

[1] ATLAS collaboration, G. Aad, *et al.*, Phys. Lett. B **716**, 1 (2012).

[2] CMS collaboration, S. Chatrchyan, *et al.*, Phys. Lett. B **716**, 30 (2012).

[3] U. Baur, T. Plehn, and D. Rainwater, Physical Review D **67**, (2003).

[4] F. Geortz, A. Papaefstathiou, L. L. Yang, and J. F. Zurita, arXiv:1309.3805v1[hep-ph] (2013).

[5] V. Barger, L. L. Everett, C. B. Jackson, and G. Shaughnessy, arXiv:1311:2931 **1**, (2013).

[6] D. E. F. de Lima, A. Papaefstathiou, and M. Spannowsky, arXiv:1404.7139v2[hep-ph] **2**, (2014).

[7] J. Baglio *et al.*, arXiv:1212.5581v2[hep-ph] **2**, (2013).

[8] C. Adolphson *et al.*, arXiv:1306.6353 **1**, (2013).

[9] H. Baer, T. Barklow, K. Fujii, Y. Gao, A. Hoang, *et al.*, **2:Physics**, (2013).

[10] T. Behnke *et al.*, **4**, (2013).

[11] D. J. Miller and S. Moretti, Eur. Phys. J.] **C 13**, 459 (2000).

[12] A. Djouadi, W. Kilian, M.Muhlleitner, and P. Zerwas, hep-ph9903229 (1999).

[13] J. Tian and K. Fujii, arXiv:1311.6528v1[hep-ph] **1**, (2013).